

# Angle dependent surface enhanced Raman scattering obtained from a Ag nanorod array substrate

Yongjun Liu, Jianguo Fan, and Y.-P. Zhao<sup>a)</sup>

Department of Physics and Astronomy, University of Georgia, Athens, Georgia 30602  
and Nanoscale Science and Engineering Center, University of Georgia, Athens, Georgia 30602

Saratchandra Shanmukh and Richard A. Dluhy

Department of Chemistry, University of Georgia, Athens, Georgia 30602  
and Nanoscale Science and Engineering Center, University of Georgia, Athens, Georgia 30602

(Received 28 July 2006; accepted 18 September 2006; published online 27 October 2006)

The angular dependence of surface enhanced Raman scattering (SERS) has been investigated for molecules adsorbed onto Ag nanorod array substrates fabricated using an oblique angle deposition technique. The strong SERS signal of *trans*-1,2-bis(4-pyridyl) ethene (BPE) was found to be strongly dependent on the incident angle of the excitation laser, with the maximum SERS intensity appearing at approximately 45° relative to the surface normal. A scattering model based on classical electrodynamic dipole radiation has been developed for BPE adsorbed onto these Ag nanorod substrates, and the theoretical SERS scattering intensity was found to be in good agreement with the experimental results. © 2006 American Institute of Physics. [DOI: 10.1063/1.2369644]

Surface enhanced Raman scattering (SERS) is a powerful and sensitive spectroscopic method for chemical structure analysis.<sup>1-4</sup> A large variety of nanostructures have been found to manifest the SERS effect, including rough metallic surfaces by electrochemical oxidation reduction cycles,<sup>5</sup> chemical etching,<sup>6</sup> and island films;<sup>7</sup> aggregates of colloidal particles;<sup>8,9</sup> high aspect ratio Ag and Au nanorods and nanowires fabricated by chemical and electrochemical methods;<sup>10,11</sup> or regular nanoparticle arrays prepared by nanosphere lithography<sup>12,13</sup> or electron-beam lithography.<sup>14</sup> Unfortunately, many of these fabrication methods are expensive or time consuming and fail to produce reproducible substrates with the correct nanostructure to provide maximum SERS enhancements.

Recently, the oblique angle deposition (OAD) technique was employed to produce nanorod arrays that were shown to make excellent SERS substrates.<sup>15-17</sup> OAD is a physical vapor deposition technique in which the incident metal vapor atoms are deposited on a substrate at a large incident angle (>70°) with respect to the surface normal of the substrate.<sup>18-20</sup> Due to the shadowing effect and surface diffusion, nanocolumnar structures can be formed. We have recently demonstrated that a Ag nanorod array fabricated by OAD with length of ~868 nm, diameter of ~99 nm, and tilting angle of 73° achieved a SERS enhancement factor of 10<sup>8</sup> for the molecular probe *trans*-1,2-bis(4-pyridyl) ethene (BPE).<sup>15,16</sup> The OAD technique can offer a flexible, easy, and inexpensive way for the fabrication of Ag nanorod arrays for high sensitivity SERS applications. In this letter, we report in our investigations of the angular dependence of the SERS scattering intensity from BPE molecules adsorbed onto Ag nanorod substrates fabricated by the OAD method. We have observed that the SERS signal from BPE molecules adsorbed onto Ag nanorod arrays shows a strong dependence on the incident angle that the excitation laser makes with the surface normal. We have theoretically modeled these results using classical dipole radiation electrodynamics from molecules adsorbed on the nanorod surface. These observations

can help to optimize the design of a SERS sample interface for these nanorod array substrates.

The Ag (Alfa Aesar, 99.999%) nanorod array substrates were prepared by OAD technique using a custom-designed electron-beam evaporation system.<sup>15</sup> The details of the deposition configuration and conditions have been reported elsewhere.<sup>15</sup> In brief, a layer of 500 nm Ag thin film was first deposited onto the glass substrate (Gold Seal® Catalog No. 3010). Then a Ag nanorod array with a length of ~1 μm was deposited using the OAD method at a vapor incident angle of 86°. A schematic of the substrate structure is illustrated in Fig. 1(a), and a typical scanning electron microscopy (SEM) image of the Ag nanorod substrate is shown in Fig. 1(b). The tilting angle  $\beta$  of the nanorods was measured to be ~73°. The nanorod substrate was mounted onto a rota-

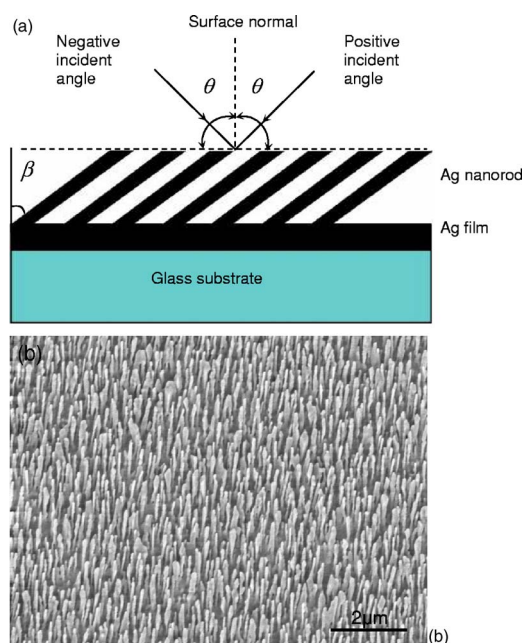


FIG. 1. (Color online) (a) Schematic illustration of the structure of the Ag nanorod array on a glass substrate and definition of the incident angles. (b) SEM image of the Ag nanorod array fabricated by the OAD technique.

<sup>a)</sup>Electronic mail: zhaoy@physast.uga.edu

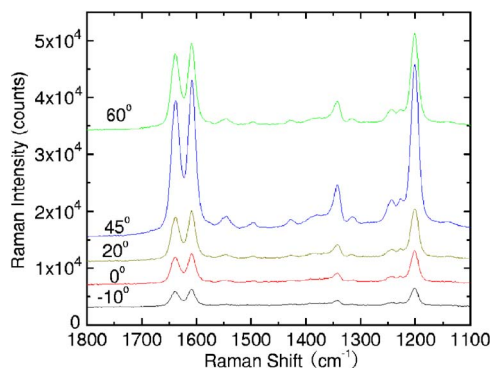


FIG. 2. (Color online) Representative SERS spectra of BPE adsorbed on the Ag nanorod substrate at different incident angles  $\theta = -10^\circ, 0^\circ, 20^\circ, 45^\circ$ , and  $60^\circ$ . The peak intensity was strongest at around  $45^\circ$ .

tion stage, facing a fiber-optic interfaced Raman probe head containing both the excitation and collection fibers. The fiber Raman system utilized was the HRC-10HT Raman analyzer from Enwave Optronics Inc. It consists of a diode laser, a spectrometer, an integrated Raman probe head used for both excitation and collection, and separate delivery and collection fibers. The excitation source is a frequency stabilized, narrow linewidth, near an IR diode laser with a wavelength of 785 nm. The excitation laser beam coupled to a 100  $\mu\text{m}$  fiber is focused onto the substrate through the Raman probe head and is unpolarized at the sample. The focal length of the Raman probe is 6 mm, and the diameter of the focal spot is 1 mm. The Raman signal from the substrate is also collected by the same Raman probe head and is coupled to a 200  $\mu\text{m}$  collecting fiber, which delivers the signal to the spectrometer equipped with a charge coupled device detector. The Raman probe molecule used in this study was *trans*-1,2-bis(4-pyridyl) ethene (Aldrich, 99.9+%). A  $10^{-6}\text{M}$  BPE solution was prepared by sequential dilution in methanol (Aldrich, HPLC grade), and a 2  $\mu\text{L}$  drop of BPE solution was placed onto the Ag nanorod substrate, where it formed a sample spot with a diameter of approximately 1.2 cm. The estimated BPE molecular coverage on the nominal surface was  $1.19 \times 10^{-3}$  ML (assuming  $7 \times 10^{14}$  molecules/ $\text{cm}^2$  in a monolayer).<sup>21</sup> Thus, approximately  $1.39 \times 10^{-14}$  moles of BPE were excited in the laser spot.

SERS spectra were collected from multiple spots on different samples in order to ensure the reproducibility and accuracy of the measurements. Since the Ag nanorod substrates used in this study are highly anisotropic [see, e.g., Fig. 1(b)], different incident laser angles can result in different Raman spectral intensities for the BPE bands, especially when the tilting plane of the Ag nanorods is parallel to the incident plane, as shown in Fig. 1(a). Therefore, one has to account for the effect of the laser incident angle on the spectral intensities. For modeling purposes, we have assigned a positive incident angle when the incident direction, is facing the nanorod tilting direction, as shown in Fig. 1(a) (first quadrant in the incident plane), while a negative incident angle is assigned when the laser strikes the surface on the other side of the surface normal (second quadrant in the incident plane). All the SERS spectra reported here were collected with an incident power of  $\sim 30$  mW and a collection time of 10 s.

Figure 2 shows the representative SERS spectra of BPE on Ag nanorod arrays at the different incident angles  $\theta = -10^\circ, 0^\circ, +20^\circ, +45^\circ$ , and  $+60^\circ$ . All the spectra show the characteristic Raman peaks of BPE; i.e., the  $1200\text{ cm}^{-1}$  peak

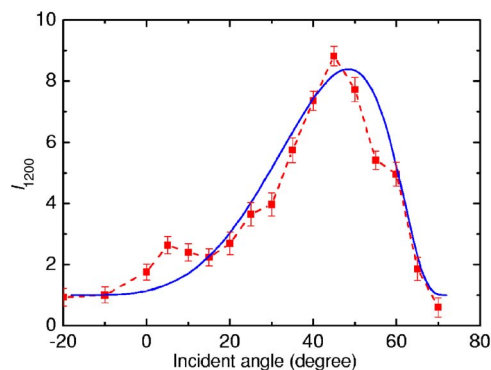


FIG. 3. (Color online) Integrated SERS intensity for the BPE band at  $1200\text{ cm}^{-1}$  plotted as a function of the incoming laser incident angle (scattered points). In addition, the ratio of Raman scattering intensity to the incident light intensity as calculated from the modified oscillating dipole model described in the text is plotted (solid curve).

corresponds to the C=C stretching mode, the  $1610\text{ cm}^{-1}$  peak corresponds to the aromatic ring stretching mode, and the  $1639\text{ cm}^{-1}$  peak corresponds to the in-plane ring mode.<sup>22</sup> These results demonstrate that even at very low BPE coverage, a Ag nanorod array prepared by the OAD method can give very high signal-to-noise ratio spectra.

Figure 2 also shows that the Raman peak intensities change with the incident angle  $\theta$ . From  $\theta = -10^\circ$  to  $\theta = +45^\circ$ , the peak intensity of each Raman band increases with an increasing value of  $\theta$ . When the incident angle exceeds  $+45^\circ$ , the Raman peak intensity decreases, reaching a minimum value at  $+70^\circ$ . This relationship is illustrated in Fig. 3 by plotting the integrated intensity of the  $1200\text{ cm}^{-1}$  band  $I_{1200}$  versus the incident angle  $\theta$ . The maximum SERS intensity is observed at about  $\theta = +45^\circ$ , and is about five times the intensity at  $\theta = 0^\circ$ . Thus, the optimum experimental configuration to ensure maximum SERS scattering response for Ag nanorod arrays is to position the incident beam at  $\theta_0 = +45^\circ$  to the substrate surface normal. Note that the optimum angle  $\theta_0$  is smaller than the nanorod tilting angle  $\beta = 73^\circ$ .

The angular dependence of the SERS response can be interpreted qualitatively using a modified Greenler model.<sup>23,24</sup> In the Greenler model, the SERS intensity is treated as proportional to the scattering intensity of a molecule adsorbed on a planar surface, and can be calculated by classical electrodynamics. The primary electric field felt by the molecule is the sum of the incident and reflected fields, which induces an oscillating dipole in the molecule. This dipole can be treated as a point source, and its radiation field and the reflection field from the surface contribute to the Raman scattering field or the secondary field. Both the primary field and the secondary field determine the strength of the Raman scattering signal. Due to the high porosity and anisotropy of the Ag nanorod arrays used in this experiment, we cannot treat the substrate as a planar surface as in the standard Greenler model. The gap between the Ag nanorods in our array configuration is approximately 177 nm,<sup>15,16</sup> which is much larger than the diameter of the BPE molecules; in addition, the nanorods have a large aspect ratio ( $\sim 10$ ). Therefore, we assume that the BPE molecules are predominately adsorbed on the side of the nanorods. According to Yang *et al.*, the long axis of the BPE molecule is always perpendicular to the adsorbed surface.<sup>22</sup> As a result, in the development of a scattering model, we treat the BPE molecule as a dipole on the Ag nanorod surface, which is

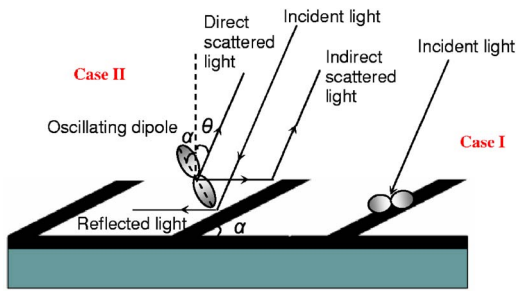


FIG. 4. (Color online) Schematic illustration of the modified Greenler's model of an induced dipole on a Ag nanorod: case I, where the dipole is perpendicular to the incident plane; case II, where the dipole is on the incident plane. All the induced dipoles are perpendicular to the nanorod.

perpendicular to the long axis of the nanorod. This arrangement is illustrated in Fig. 4.

Since the nanorods are of the same size ( $\sim 800\text{--}900\text{ nm}$ ) as the wavelength of the excitation source ( $785\text{ nm}$ ), one can as a first approximation treat the surface of the nanorod as a planar surface by neglecting the diffraction effect. Rigorously, of course, diffraction effects need to be taken into consideration since the separation and diameter of the nanorods are much smaller than the wavelength of the excitation source. However, due to the random arrangement of the nanorods on the surface, the phase coherence only exists at a short distance and disappears at a long distance. In order to calculate the Raman scattering field, we consider two dipole configurations: case I, where the dipole is perpendicular to the incident plane, and case II, where the dipole is in the incident plane, as shown in Fig. 4. Since the Raman signal in the experiments was collected through a backscattering configuration, we only consider the backscattered Raman signal in the model. The oscillating dipole excited by incident light can be considered as a point source emitting radiation from the side wall of the nanorod. For case I, only the  $s$ -polarized incident light can induce a dipole radiation, and the scattered Raman field collected by the detector is a constant since the collecting direction is always perpendicular to the induced dipole oscillation direction. For case II, only the  $p$ -polarized light can induce dipole oscillation. Due to the tilting of the nanorods, only dipoles on one side of the nanorods can be excited, as shown in Fig. 4. The total Raman scattering field  $E_p$  is the sum of the scattered field radiated directly from the dipole, namely, the "direct scattered field" in Fig. 4, and that reflected from the nanorod surface, namely, the "indirect scattered field" in Fig. 4,

$$\langle E_p^2 \rangle / \langle E_i^2 \rangle \sim (1 + R_p + 2\sqrt{R_p} \cos \delta_p)^2 \sin^4(\theta_i), \quad (1)$$

where  $E_i$  is the incident field,  $\theta_i = \alpha + \theta$  is the incident angle on the nanorod,  $\alpha = 90^\circ - \beta$ , and  $\theta$  is the incident angle with respect to surface normal of substrate.  $R_p = |r_p|^2$ ,  $\delta_p = \tan^{-1}(\text{Im}(r_p)/\text{Re}(r_p))$ . The  $r_p$  is the reflectivity of  $p$ -polarized light on Ag surface, determined by the Fresnel equations,<sup>25</sup>

$$r_p = [n_2^2 \cos \theta_i - n_1(n_2^2 - n_1^2 \sin^2 \theta_i)^{1/2}] / [n_2^2 \cos \theta_i + n_1(n_2^2 - n_1^2 \sin^2 \theta_i)^{1/2}], \quad (2)$$

where  $n_1 = 1$  and  $n_2 = 0.03 + 5.242i$  are the indices of refraction of air and Ag at the wavelength of  $785\text{ nm}$ , respectively. Considering both cases I and II, the total Raman scattering field  $E_{R\text{-total}}$  can be written as

$$\langle E_{R\text{-total}}^2 \rangle / \langle E_i^2 \rangle \sim (1 + R_p + 2\sqrt{R_p} \cos \delta_p)^2 \sin^4(\theta_i) + 1. \quad (3)$$

The solid curve plotted in Fig. 3 is a result of theoretical calculations obtained from the modified Greenler model in Eq. (1) by assuming  $\alpha = 17^\circ$ . The curve is rescaled in order to match the experimental data. Both the experimental data and the theoretic curve show asymmetric angular dependence, with a maximum observed SERS scattering intensity expected at  $45^\circ\text{--}50^\circ$  relative to the surface normal. At negative incident angles, the model predicts that the Raman intensity should approach a constant value, which is consistent with the experimental data. Overall, the model provides a good agreement with the observed SERS intensities for the BPE molecule adsorbed on Ag nanorods.

In conclusion, SERS scattering from BPE molecules adsorbed onto Ag nanorod substrates prepared by an OAD technique has been shown to be strongly dependent upon the incident angle of the incoming laser beam. This behavior can be qualitatively explained by a modified Greenler model by considering the anisotropic nature of the Ag nanorods.

Three of the authors (Y.J.L., J.G.F., and Y.P.Z.) thank the support from the National Science Foundation (Grant No. ECS0304340) and Georgia Research Alliance Technology Catalyst Award. Two of the authors (S.S.) and (R.A.D.) are supported by the U.S. Public Health Service through the National Institute of Health (Grant No. EB001956).

- <sup>1</sup>T. Vo-Dinh, *Trends Analyt. Chem.* **17**, 557 (1998).
- <sup>2</sup>Z. Q. Tian, B. Ren, and D. Y. Wu, *J. Phys. Chem. B* **106**, 9463 (2002).
- <sup>3</sup>K. Kneipp, H. Kneipp, I. Itzkan, R. R. Dasari, and M. S. Feld, *J. Phys.: Condens. Matter* **14**, R597 (2002).
- <sup>4</sup>J. A. Dieringer, O. Lyandres, X. Zhang and R. P. Van Duyne, *Faraday Discuss.* **132**, 9 (2006).
- <sup>5</sup>J. E. Pemberton, in *Electrochemical Interfaces Modern Techniques for In-Situ Characterization*, edited by H. D. Abruna (VCH, Berlin, 1991), pp. 195–263.
- <sup>6</sup>K. T. Carron, X. Gi, and M. L. Lewis, *Langmuir* **7**, 2 (1991).
- <sup>7</sup>V. L. Schlegel and T. M. Cotton, *Anal. Chem.* **63**, 241 (1991).
- <sup>8</sup>S. M. Nie and S. R. Emery, *Science* **275**, 1102 (1997).
- <sup>9</sup>K. Kneipp, Y. Wang, H. Kneipp, L. T. Perelman, I. Itzkan, R. Dasari, and M. S. Feld, *Phys. Rev. Lett.* **78**, 1667 (1997).
- <sup>10</sup>B. Nikoobakht and M. A. El-Sayed, *J. Phys. Chem. A* **107**, 3372 (2003).
- <sup>11</sup>A. Tao, F. Kim, C. Hess, J. Goldberger, R. R. He, Y. G. Sun, Y. N. Xia, and P. D. Yang, *Nano Lett.* **3**, 1229 (2003).
- <sup>12</sup>C. L. Haynes and R. P. Van Duyne, *J. Phys. Chem. B* **105**, 5599 (2001).
- <sup>13</sup>T. R. Jensen, M. D. Malinsky, C. L. Haynes, and R. P. Van Duyne, *J. Phys. Chem. B* **104**, 10549 (2000).
- <sup>14</sup>N. Felidj, J. Aubard, G. Levi, J. R. Krenn, A. Hohenau, G. Schider, A. Leitner, and F. R. Aussenegg, *Appl. Phys. Lett.* **82**, 3095 (2003).
- <sup>15</sup>S. B. Chaney, S. Shanmukh, R. A. Duluhy, and Y.-P. Zhao, *Appl. Phys. Lett.* **87**, 031908 (2005).
- <sup>16</sup>Y.-P. Zhao, S. B. Chaney, S. Shanmukh, and R. A. Duluhy, *J. Phys. Chem. B* **110**, 3153 (2006).
- <sup>17</sup>J.-G. Fan and Y.-P. Zhao, *J. Vac. Sci. Technol. B* **23**, 947 (2005).
- <sup>18</sup>L. Abelmann and C. Lodder, *Thin Solid Films* **305**, 1 (1997).
- <sup>19</sup>R. N. Trait, T. Smy, and M. J. Brett, *Thin Solid Films* **226**, 196 (1993).
- <sup>20</sup>Y.-P. Zhao, D.-X. Ye, G.-C. Wang, and T.-M. Lu, *Proc. SPIE* **5219**, 59 (2003).
- <sup>21</sup>K. L. Norrod, L. M. Sudnik, D. Rousell, and K. L. Rowlen, *Appl. Spectrosc.* **51**, 994 (1997).
- <sup>22</sup>W.-H. Yang, J. Hulteen, G. C. Schatz, and R. P. Van Duyne, *J. Chem. Phys.* **104**, 4313 (1996).
- <sup>23</sup>R. G. Greenler and T. C. Slager, *Spectrochim. Acta, Part A* **29A**, 191 (1973).
- <sup>24</sup>A. Campion, in *Vibrational Spectroscopy of Molecules on Surface*, edited by J. T. Yates, Jr. and T. E. Madey (Plenum, New York, 1987), Ch. 5, pp. 360–369.
- <sup>25</sup>M. Born and E. Wolf, *Principles of Optics*, 6th ed. (Cambridge University Press, Cambridge, 1980), pp. 36–45.